Absence of actual plateaus in zero-temperature magnetization curves of quantum spin clusters and chains

Vadim Ohanyan,[1,2] Onofre Rojas,[2,3] Jozef Strečka,[4] and Stefano Bellucci[5]

[1]*Department of Theoretical Physics, Yerevan State University, Alex Manoogian 1, 0025 Yerevan, Armenia*

[2]*ICTP, Strada Costiera 11, I-34151 Trieste, Italy*

[3]*Departamento de Fisica, Universidade Federal de Lavras, CP 3037, 37200000, Lavras, MG, Brazil*

[4]*Department of Theoretical Physics and Astrophysics, Faculty of Science, P. J. Šafárik University, Park Angelinum 9, 040 01, Košice, Slovak Republic*

[5]*INFN-Laboratori Nazionali di Frascati, Via E. Fermi 40, 00044 Frascati, Italy*

(Received 10 June 2015; revised manuscript received 22 September 2015; published 16 December 2015)

We examine the general features of the noncommutativity of the magnetization operator and Hamiltonian for small quantum spin clusters. The source of this noncommutativity can be a difference in the Landé g factors for different spins in the cluster, XY anisotropy in the exchange interaction, and the presence of the Dzyaloshinskii-Moriya term in a direction different from the direction of the magnetic field. As a result, zero-temperature magnetization curves for small spin clusters mimic those for the macroscopic systems with the band(s) of magnetic excitations, i.e., for the given eigenstate of the spin cluster the corresponding magnetic moment can be an explicit function of the external magnetic field yielding the nonconstant (nonplateau) form of the magnetization curve within the given eigenstate. In addition, the XY anisotropy makes the saturated magnetization (the eigenstate when all spins in cluster are aligned along the magnetic field) inaccessible for finite magnetic field magnitude (asymptotical saturation). We demonstrate all these features on three examples: a spin-1/2 dimer, mixed spin-(1/2,1) dimer, and a spin-1/2 ring trimer. We consider also the simplest Ising-Heisenberg chain, the Ising-XYZ diamond chain, with four different g factors. In the chain model the magnetization curve has a more complicated and nontrivial structure than that for clusters.

DOI: 10.1103/PhysRevB.92.214423 PACS number(s): 75.10.Pq, 75.50.Xx

I. INTRODUCTION

Magnetization curves of low-dimensional quantum antiferromagnets are topical issues of current research interest, because they often involve intriguing features such as magnetization plateaus, jumps, ramps, and/or kinks. The spin-1/2 quantum Heisenberg chain, the spin-1/2 quantum Ising chain in a transverse field, and the spin-1/2 quantum XX chain in a transverse field are a few paradigmatic examples of exactly solved quantum spin chains for which zero-temperature magnetization varies smoothly with rising magnetic field until the saturation magnetization is reached [1–3]. Contrary to this, the integer-value quantum Heisenberg chains (and also many other low-dimensional quantum antiferromagnets) contain in a zero-temperature magnetization process remarkable magnetization plateau(s) at rational value(s) of the saturation magnetization [4,5]. The intermediate plateaus of Heisenberg spin chains reflect quantum states of matter with exotic topological order such as the Haldane phase [6,7], whereas their presence is restricted by the quantization condition known as Oshikawa-Yamanaka-Affleck rule [8,9].

On the other hand, it could be generally expected that the antiferromagnetic Heisenberg spin clusters should always exhibit leastwise one intermediate plateau before the magnetization jumps to its saturation value [10–13]. This naive expectation follows from the energy spectrum of the quantum Heisenberg spin clusters, which are composed of a few discrete energy levels that cannot naturally form a continuous energy band needed for a smooth variation of the magnetization at zero temperature. At first sight, this argumentation is consistent with the existence of at least one plateau and magnetization jump, which bears a close relation to level crossing caused by the external magnetic field. From this perspective, the quite natural question arises as to whether or not intermediate magnetization plateau(s) can be partially or completely lifted from zero-temperature magnetization curves of the Heisenberg spin clusters.

Other spin systems which should be noted in the context of the small quantum spin clusters are the Ising-Heisenberg chains. They are the one-dimensional spin systems where the small quantum spin clusters are assembled to the chain by alternating with the Ising spins in such a way that the Hamiltonian for the whole system is a sum of mutually commuting block Hamiltonians. These systems have much in common with the "classical" chains of the Ising spins, as they can be solved by the same technique and the eigenstates are just the direct product of the eigenstates of the single block, though, for the more complicated structure doubling of the unit cell is possible. Thus the magnetization curves for the Ising-Heisenberg spin systems share almost all features with the magnetization curves of the small spin clusters but can contain much more intermediate magnetization plateaus. Various variants of the Ising-Heisenberg chains have been examined: diamond chain [14–28], sawtooth chain [29,30], orthogonal-dimer chain [31–33], tetrahedral chain [34–38], and some special examples relevant to real magnetic materials [39–42].

In the present work, we will rigorously examine a magnetization process of a few quantum Heisenberg spin clusters and the Ising-Heisenberg diamond chain, which will not display strict magnetization plateaus on the assumption that some constituent spins have different Landé g factors and may be an XY anisotropy of the exchange interaction. Also, the Dzyaloshinskii-Moriya (DM) term in a direction different from

that of the magnetic field can lead to the same effect. All those features of the spin Hamiltonian make the magnetization nonconserved, i.e., noncommutating with the Hamiltonian. This specific requirement naturally leads to a nonlinear dependence of the energy levels on a magnetic field, which consequently causes a smooth change of the magnetization with the magnetic field within one and the same eigenstate. Although the smooth change of magnetization due to a difference in Landé g factors or/and XY anisotropy and the noncollinear DM term may be quite reminiscent of that of quantum spin chains with continuous energy bands, it is, of course, of a completely different mechanism with a much simpler origin.

The single-chain magnet, $[\{(CuL)_2Dy\}\{Mo(CN)_8\}] \cdot 2CH_3CN \cdot H_2O$ [40–42], is a remarkable example of both an Ising-Heisenberg one-dimensional spin system and a spin model with different Landé g factors, leading to a nonplateau form of the region of the magnetization curve corresponding to the same eigenstate. However, as the exact analysis shows [42], the effect is just barely visible in the magnetization curve plot by virtue of the very small difference in Landé g factors of the magnetic ions, although the exact expression for the magnetization has explicit dependence on the magnetic field. Almost the same effect but even quantitatively less pronounced has been observed in the approximate model of the one-dimensional magnet, the F-F-AF-AF spin chain compound Cu(3-chloropyridine)$_2$(N$_3$)$_2$ [39].

The organization of this paper is as follows. In the next section, we clarify a few general statements closely related to the absence of actual plateaus in zero-temperature magnetization curves of quantum spin clusters and chains. These arguments of general validity will be subsequently illustrated on a few specific examples of the spin-1/2 quantum Heisenberg dimer, the mixed spin-(1/2,1) Heisenberg dimer, the spin-1/2 Heisenberg trimer, and the spin-1/2 Ising-Heisenberg diamond chain in the following four sections. A summary of the most important findings along with the implications for experimental systems will be presented in the concluding part.

II. GENERAL STATEMENTS

Let us first start with a few very general statements elucidating the issue of the nonconstant magnetization within one physical state or the explicit magnetic field dependence of the magnetization corresponding to a certain eigenstate of the small spin clusters. Obviously, the aforementioned phenomenon arises when the magnetization is not a good quantum number,

$$[\mathcal{H},\, \mathcal{M}^z] \neq 0. \tag{1}$$

Here, $\mathcal{H}$ stands for the Hamiltonian of a spin cluster. One can distinguish two cases, when the z projection of the total spin $S^z_{\rm tot}$ does not commute with the Hamiltonian and the magnetization operator is proportional to it,

$$\left[\mathcal{H},\, S^z_{\rm tot}\right] \neq 0, \quad \mathcal{M}^z = g\mu_B S^z_{\rm tot}, \tag{2}$$

or when the z projection of the total spin $S^z_{\rm tot}$ is a good quantum number, but the magnetization operator is not proportional to it and does not commute with the Hamiltonian,

$$\left[\mathcal{H},\, S^z_{\rm tot}\right] = 0, \quad \mathcal{M}^z \neq g\mu_B S^z_{\rm tot}. \tag{3}$$

Of course, another possibility is to have the magnetization which is nonproportional to $S^z_{\rm tot}$ and the z projection of the total spin $S^z_{\rm tot}$ nonconserved. The spin Hamiltonians, which do not commute with $S^z_{\rm tot}$, usually contain XY anisotropy or/and a DM vector with a nonzero X or Y part. The magnetization is nonproportional to the total spin $S^z_{\rm tot}$ when the spins possess different Landé g factors.

III. SPIN-1/2 HEISENBERG DIMER

In this section we consider the spin-1/2 Heisenberg dimer as the simplest system of two interacting quantum spins described by the most general Hamiltonian

$$\begin{aligned}\mathcal{H}_{\rm dim} = {} & J\left\{(1+\gamma)S^x_1 S^x_2 + (1-\gamma)S^y_1 S^y_2 + \Delta S^z_1 S^z_2\right\} \\ & + \mathbf{D}\cdot(\mathbf{S}_1 \times \mathbf{S}_2) - \mathbf{B}\cdot(g_1\boldsymbol{S}_1 + g_2\boldsymbol{S}_2).\end{aligned} \tag{4}$$

Here, $S^\alpha_{1,2}$, $(\alpha = x,y,z)$ are the spatial components of the spin-1/2 operators for two spins in the dimer. We assume the fully anisotropic XYZ Heisenberg coupling with two anisotropy constants γ, Δ and two different but isotropic Landé g factors. The spatial direction of the magnetic field $\boldsymbol{B}$ and the DM-vector $\boldsymbol{D}$ are arbitrary so far. Without loss of generality, one may, however, choose a direction of the magnetic field along the z axis and the DM vector to lie in xz plane:

$$\begin{aligned}\mathcal{H}_{\rm dim} = {} & J\left\{(1+\gamma)S^x_1 S^x_2 + (1-\gamma)S^y_1 S^y_2 + \Delta S^z_1 S^z_2\right\} \\ & + D_x\left(S^y_1 S^z_2 - S^z_1 S^y_2\right) + D_z\left(S^x_1 S^y_2 - S^y_1 S^x_2\right) \\ & - B\left(g_1 S^z_1 + g_2 S^z_2\right).\end{aligned} \tag{5}$$

Let us calculate the commutators of the Hamiltonian (5) with the z projections of the operators corresponding to the total spin and magnetization:

$$S^z_{\rm tot} = S^z_1 + S^z_2, \quad \mathcal{M}^z = g_1 S^z_1 + g_2 S^z_2, \tag{6}$$

$$\begin{aligned}[\mathcal{H}_{\rm dim}, S^z] &= -2i\gamma\left(S^x_1 S^y_2 + S^y_1 S^x_2\right) + iD_x\left(S^x_1 S^z_2 - S^z_1 S^x_2\right), \\ [\mathcal{H}_{\rm dim}, \mathcal{M}^z] &= -ig_- D_z\left(S^x_1 S^x_2 + S^y_1 S^y_2\right) \\ &\quad + ig_- J\left(S^x_1 S^y_2 - S^y_1 S^x_2\right) - i\gamma g_+\left(S^x_1 S^y_2 + S^y_1 S^x_2\right) \\ &\quad + iD_x\left(g_1 S^x_1 S^z_2 - g_2 S^z_1 S^x_2\right),\end{aligned} \tag{7}$$

where $g_\pm = g_1 \pm g_2$. As one can see, the XY anisotropy γ and the DM vector x projection D_x make the $S^z_{\rm tot}$ and $\mathcal{M}^z$ nonconserved, but even if we set them to zero, the magnetization may still be a nonconserved quantity because of the difference in Landé g factors. Thus, the spin-1/2 Heisenberg dimer may exhibit the nonconstant magnetization within one ground state if at least one of the parameters, $g_2 - g_1$, γ, or $D_x(D_y)$ is nonzero. Let us put $D_x = 0$ as it makes the analytic calculations quite cumbersome (the eigenvalue problem leads to a quartic equation), and start with the exact diagonalization of the Hamiltonian for the anisotropic spin-1/2 Heisenberg dimer with different Landé g factors. The eigenvalues are

$$\begin{aligned}\varepsilon_{1,2} &= -\frac{J\Delta}{4} \pm \frac{1}{2}\sqrt{B^2 g_-^2 + J^2 + D_z^2}, \\ \varepsilon_{3,4} &= \frac{J\Delta}{4} \pm \frac{1}{2}\sqrt{B^2 g_+^2 + J^2\gamma^2}.\end{aligned} \tag{8}$$

The corresponding eigenvectors are

$$|\Psi_{1,2}\rangle = \frac{1}{\sqrt{1+|A_\pm|^2}}(|\uparrow\downarrow\rangle + A_\pm|\downarrow\uparrow\rangle),$$
$$A_\pm = \rho_\pm e^{i\phi}, \quad \phi = \arctan\frac{D_z}{J},$$
$$\rho_\pm = \frac{Bg_- \pm \sqrt{B^2g_-^2 + J^2 + D_z^2}}{\sqrt{J^2+D_z^2}}, \tag{9}$$
$$|\Psi_{3,4}\rangle = \frac{1}{\sqrt{1+B_\pm^2}}(|\uparrow\uparrow\rangle + B_\pm|\downarrow\downarrow\rangle),$$
$$B_\pm = \frac{Bg_+ \pm \sqrt{B^2g_+^2 + J^2\gamma^2}}{J\gamma}.$$

Under the conditions $g_1 = g_2$ (and $D_z = 0$) the first two eigenstates become conventional singlet and a $S^z_{\rm tot} = 0$ component of the triplet, respectively. However, there is no continuous transition to the $S^z_{\rm tot} = 1$ and $S^z_{\rm tot} = -1$ components of the triplet in $|\Psi_{3,4}\rangle$ at $\gamma \to 0$. In order to obtain $|\uparrow\uparrow\rangle$ and $|\downarrow\downarrow\rangle$, one has to put $\gamma = 0$ in the Hamiltonian before diagonalization. Let us calculate the magnetization eigenvalues for all those eigenstates:

$$\langle\Psi_{1,2}|\left(g_1S_1^z + g_2S_2^z\right)|\Psi_{1,2}\rangle = \frac{1}{2}g_-\frac{1-\rho_\pm^2}{1+\rho_\pm^2} = \mp\frac{Bg_-^2}{2\sqrt{B^2g_-^2 + J^2 + D_z^2}} \tag{10}$$

At $g_1 = g_2$ this expression becomes 0. However, at $g_1 \neq g_2$ we have explicit dependence of the eigenvalue, corresponding to the certain eigenstate on the magnetic field. This leads to a nonconstant magnetization for the given eigenstate. Thus, we have here $S^z_{\rm tot} = 0$ and $\mathcal{M}^z \neq 0$.

For the other two eigenstates we have

$$\langle\Psi_{3,4}|\left(g_1S_1^z + g_2S_2^z\right)|\Psi_{3,4}\rangle = \frac{1}{2}g_+\frac{1-B_\pm^2}{1+B_\pm^2} = \mp\frac{Bg_+^2}{2\sqrt{B^2g_+^2 + J^2\gamma^2}}. \tag{11}$$

At $\gamma = 0$ the expression transforms to

$$\langle\Psi_{3,4}|\left(g_1S_1^z + g_2S_2^z\right)|\Psi_{3,4}\rangle = \mp\tfrac{1}{2}g_+, \tag{12}$$

which corresponds to $|\uparrow\uparrow\rangle$ and $|\downarrow\downarrow\rangle$ eigenstates. Equation (11) has another important feature. The transverse quantum fluctuations enhanced by the XY anisotropy γ reduce the magnetization in z direction in such a way that it never reaches its saturated values $\pm\frac{1}{2}(g_1+g_2)$ at any nonzero γ and finite magnetic field B. It is also important that even at the equal g factors, $g_2 = g_1 = g$, the magnetization expectation values for the eigenstates $|\Psi_{3,4}\rangle$ exhibit explicit magnetic field dependence and do not reach their saturated values at nonzero γ. Another case of interest is the $g_2 = -g_1 = g$, when the magnetization expectation value for the $|\Psi_{1,2}\rangle$ is nonzero and exhibits explicit dependence on the magnetic field and the eigenstates $|\Psi_{3,4}\rangle$ demonstrate zero magnetization. Moreover, the corresponding expectation values become singular at $\gamma = 0$, because, as was mentioned above, there is no continuous limit $\gamma \to 0$ in terms of eigenvalues and eigenvectors. The magnetic susceptibility for the aforementioned states can be obtained in a straightforward way by taking a derivative of Eqs. (10) and (11) with respect to $\mp B$:

$$\mp\frac{\partial}{\partial B}\langle\Psi_{1,2}|\left(g_1S_1^z + g_2S_2^z\right)|\Psi_{1,2}\rangle = \frac{J^2g_-^2}{2\sqrt{\left(B^2g_-^2 + J^2\right)^3}},$$
$$\mp\frac{\partial}{\partial B}\langle\Psi_{3,4}|\left(g_1S_1^z + g_2S_2^z\right)|\Psi_{3,4}\rangle = \frac{J^2\gamma^2g_+^2}{2\sqrt{(B^2g_+^2 + J^2\gamma^2)^3}}. \tag{13}$$

The deviation from the horizontal line for the zero-temperature magnetization curve of the dimer under consideration is thus governed by three factors. The difference of Landé g factors, $g_2 - g_1$, is responsible for the nonplateau behavior for the initial part of the magnetization curve, and as $B \leqslant B_c$, the larger the absolute value of the difference the more pronounced the deviation is. At the same time, the overall Landé g factor, $g_1 + g_2$, and the XY anisotropy γ make another part of the magnetization curve, which in the limit $\gamma = 0$ corresponds to the saturation $|\uparrow\uparrow\rangle$, nonflat. The critical field B_c is found from the level crossing. As for the zero temperature where only $|\Psi_2\rangle$ and $|\Psi_4\rangle$ are realized, we can find the corresponding value of the magnetic field from the equation $\varepsilon_2 = \varepsilon_4$, which leads to

$$B_c = \frac{\sqrt{2g_1g_2\Gamma_- + J\Delta\left\{\left(g_1^2+g_2^2\right)J\Delta + \sqrt{4g_1^2g_2^2\left[\left(g_1^2+g_2^2\right)\Gamma_- + 2g_1g_2\Gamma_+\right] + \left(g_1^2-g_2^2\right)^2J^2\Delta^2}\right\}}}{2\sqrt{2}g_1g_2}, \tag{14}$$

with

$$\Gamma_\pm = \left[D_z^2 + J^2(1\pm\gamma^2)\right]. \tag{15}$$

The typical picture of the level crossing curve one can see in Fig. 1. However, the $B = 0$ ground state is also affected by the value of the XY anisotropy γ. The ground state becomes $|\Psi_4\rangle$ for a sufficiently large γ above a certain critical value γ_c. The critical value is given by the equation

$$\gamma_c = \Delta + \sqrt{1 + (D_z/J)^2}. \tag{16}$$

The nonlinear behavior with respect to the magnetic field is the main reason for the nonplateau magnetization. As the DM term in z direction does not bring any qualitatively new physics, we can hereafter put $D_z = 0$. The expression for the critical field (14) does not lead to a proper $\gamma = 0$ limit. The case of isotropic

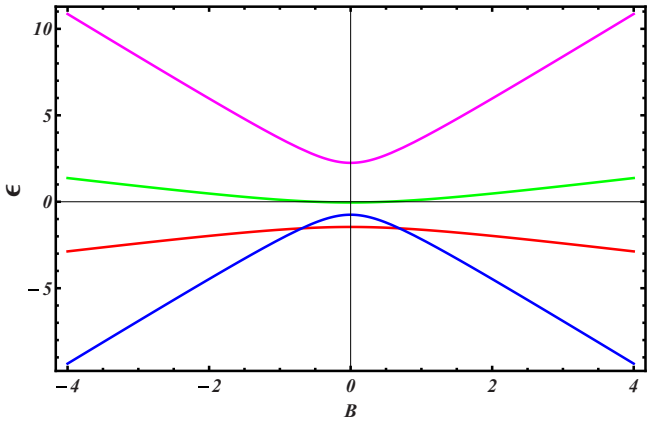

FIG. 1. (Color online) The energy spectrum of the isolated $S = 1/2$ dimer with $g_1 = 2$, $g_2 = 3$, $J = 1$, $D_z = 1$, $\gamma = 2$, and $\Delta = 3$ displaying level crossing. The two bottom curves correspond to ε_2 and ε_4. The nonlinearity in B on the energy levels is the main reason for the nonplateau magnetization.

Heisenberg interaction must be considered separately. In the case of isotropic Heisenberg interaction the difference is only in the saturated states presented here, which transforms to $|\Psi_{3,4}\rangle$ at nonzero γ, while the $|\Psi_{1,2}\rangle$ eigenstates remain the same. The value of critical field in this case is

$$B_c = J\frac{g_+\Delta + \sqrt{g_-^2\Delta^2 + 4g_1g_2}}{4g_1g_2}. \quad (17)$$

Thus, the jump to the saturated magnetization takes place for $\gamma = 0$ at this value of the magnetic field. The magnitude of the jump depends on the difference of the Landé g factors and is given by

$$\Delta M = \frac{g_+}{2}\left\{1 - \frac{g_-^2\left[\Delta + \frac{\sqrt{g_-^2\Delta^2+4g_1g_2}}{g_+}\right]}{4g_1g_2\sqrt{1 + \frac{g_-^2[g_+\Delta+\sqrt{g_-^2\Delta^2+4g_1g_2}]}{16g_1^2g_2^2}}}\right\}. \quad (18)$$

The corresponding plots of the zero-temperature magnetization one can find in Figs. 2 and 3. In Fig. 2 the evolution of the $T = 0$ ground state for different values of γ are presented for $J = 1$, $D_z = 1$, $\Delta = 2$, $g_1 = 2$, and $g_2 = 6$. The critical value of γ at which the $B = 0$ ground state of the spin-1/2 spin dimer changes from $|\Psi_2\rangle$ to $|\Psi_4\rangle$ for these values of J, D_z and Δ is $\gamma_c = 2 + \sqrt{2} \simeq 3.41$. Therefore, for $\gamma = 0$ and $\gamma = 2$ one can see magnetization curves with two eigenstates separated by the jump. The nonplateau behavior of the magnetization for $|\Psi_2\rangle$ at $B < B_c$ is well visible. Also, the nonplateau character of the magnetization curve corresponding to $|\Psi_4\rangle$ is obvious for $\gamma = 2$, while for $\gamma = 0$ we see an ideal plateau at $M = \frac{1}{2}(g_1 + g_2) = 4$. This nonplateau behavior and inaccessibility of the saturation are more pronounced for $\gamma = 2$ and $\gamma = 4$ when the system for all values of the magnetic field ($B > 0$) is in the $|\Psi_4\rangle$ eigenstate, and its $T = 0$ magnetization curve demonstrates a form very similar to that of a system with a band of magnetic excitations or/and to the high-temperature magnetization curve given by the Brillouin function. The effect of the difference between the Landé g factor is summarized in Fig. 3. To demonstrate

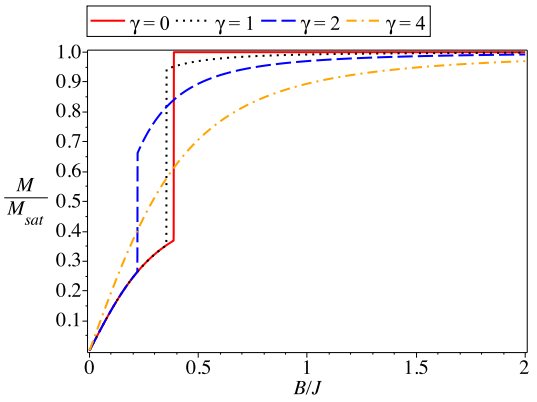

FIG. 2. (Color online) The zero-temperature magnetization curves for the $S = 1/2$ dimer with $g_1 = 2$, $g_2 = 6$, $J = 1$, $D_z = 1$, $\Delta = 2$, and $\gamma = 0$ (red, solid); $\gamma = 1$ (black, dotted); $\gamma = 2$ (blue, dashed); and $\gamma = 4$ (orange, dot-dashed). $M_{\rm sat} = \frac{1}{2}(g_1 + g_2) = 4$.

the evolution of the ground state $|\Psi_2\rangle$ under the change of the difference of Landé g factors, we have chosen $\gamma = 0$ and $J = 1, D_z = 0, \Delta = 1$ and plotted the normalized magnetization $M/M_{\rm sat}$, as the saturation magnetization, $M_{\rm sat} = \frac{1}{2}(g_1 + g_2)$, is different for each curve. For the $g_1 = g_2$ curve there are just two ideal plateaus at $M = 0$ (singlet state) and $M = 1$. The magnetization jumps from 0 to 1 at $B_c = J\frac{1+\Delta}{2g}$ (here $g_1 = g_2 = g$). However, the essential changes appear when the difference between g factors is growing. For $g_2 - g_1$ nonequal to zero the part of the magnetization curve corresponding to $S_1^z + S_2^z = 0$ deviates from the horizontal line and becomes almost linear (for small g_-), and then grows more and more rapidly with the shift of the transition point between $|\Psi_2\rangle$ and $|\Psi_4\rangle$ in the lower B region.

Of course, the effects of the DM terms in molecular magnets and other low-dimensional many-body spin systems have been

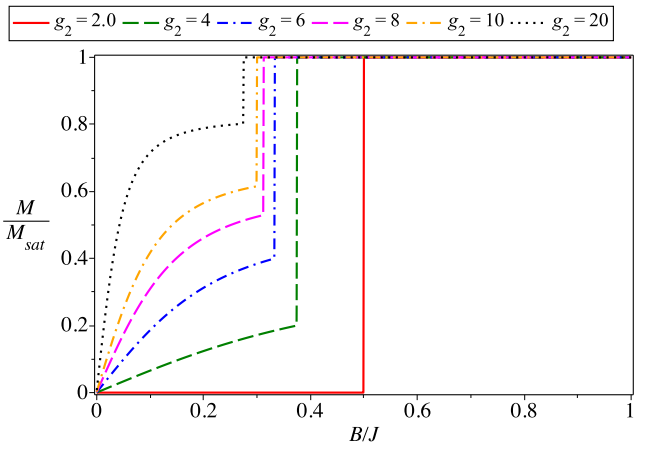

FIG. 3. (Color online) The normalized zero-temperature magnetization curves $M/M_{\rm sat}$ of the $S = 1/2$ dimer with two different g factors in case of isotropic exchange interaction, $\gamma = 0$ and $\Delta = 1$. Here, for the sake of simplicity, we put $J = 1, D_z = 0, g_1 = 2$ and present the curves for the different values of g_2. From the bottom to top $g_2 = 2$ (red); 4 (green); 6 (blue); 8 (magenta); 10 (orange); and 20 (black). $M_{\rm sat} = \frac{1}{2}(g_1 + g_2)$.

intensively studied in various contexts during the last decade [43–47]. In Ref. [44] the isolated spin dimer with DM terms has been considered with general mutual orientation of the DM vector and magnetic field,

$$\mathcal{H} = J\,\mathbf{S}_1\cdot\mathbf{S}_2 + \mathbf{D}\cdot(\mathbf{S}_1\times\mathbf{S}_2) - gB\left(S_1^z + S_2^z\right), \tag{19}$$

where $\mathbf{D} = (0, D\sin\theta, D\cos\theta)$. Though, as was shown above, in this case the eigenvalue problem leads to the solution of a quartic equation, the authors found an approximate ground state in the limit $D/J \ll 1$ and below the critical field $B = J/g$. They explicitly found out the magnetization of the ground state which turned out to be linear in B:

$$\mathbf{M} = \frac{g}{4J^3}(\mathbf{D}\times\mathbf{B})\times\mathbf{D}. \tag{20}$$

This is the approximate form of the nonlinear behavior of the magnetization we have obtained exactly above in the case of $\mathbf{D} = (0,0,D_z)$. Despite all of these results, the issue of the nonconserving magnetization and its consequences has not been systematically investigated so far.

It is also straightforward to construct the thermodynamics of the isolated dimer. The partition function is calculated directly from the spectrum:

$$Z_{\rm dim} = 2\left\{e^{\beta\frac{J\Delta}{4}}\,\mathrm{ch}\left[\frac{\beta}{2}\sqrt{B^2g_-^2 + J^2 + D_Z^2}\right] + e^{-\beta\frac{J\Delta}{4}}\,\mathrm{ch}\left[\frac{\beta}{2}\sqrt{B^2g_+^2 + J^2\gamma^2}\right]\right\}. \tag{21}$$

The magnetization is found in a standard way, as $M_{\rm dim} = \frac{1}{\beta}\left(\frac{\partial\log Z_{\rm dim}}{\partial B}\right)_\beta$, yielding

$$M_{\rm dim} = \frac{B}{Z_{\rm dim}}\left\{\frac{g_+^2 e^{-\beta\frac{J\Delta}{4}}}{\sqrt{B^2g_-^2 + J^2\gamma^2}}\,\mathrm{sh}\left[\frac{\beta\sqrt{B^2g_+^2 + J^2\gamma^2}}{2}\right] + \frac{g_-^2 e^{\beta\frac{J\Delta}{4}}}{\sqrt{B^2g_-^2 + J^2 + D_Z^2}}\,\mathrm{sh}\left[\frac{\beta\sqrt{B^2g_-^2 + J^2 + D_Z^2}}{2}\right]\right\}. \tag{22}$$

The plots of the finite-temperature magnetization for the $S = 1/2$ spin dimer are presented in Fig. 4. It is worth mentioning that thermal fluctuations eliminate from magnetization curves all typical structures (such as plateaus or quasiplateaus), quite similarly to the way large XY anisotropy does for zero-temperature magnetization curves.

IV. MIXED-SPIN HEISENBERG DIMER

Another interesting example of a simple quantum spin system, which may possibly show a striking dependence of the total magnetization on a magnetic field, is the mixed spin-(1/2,1) Heisenberg dimer defined by the Hamiltonian

$$\mathcal{H}_{\rm mixed} = J\left(S_1^x\mu_2^x + S_1^y\mu_2^y + \Delta S_1^z\mu_2^z\right) + D\left(\mu_2^z\right)^2 - B\left(g_1S_1^z + g_2\mu_2^z\right). \tag{23}$$

Here, S_1^α and μ_2^α ($\alpha = x,y,z$) represent spatial components of the spin-1/2 and spin-1 operators, respectively, the exchange constant J denotes the XXZ Heisenberg coupling between

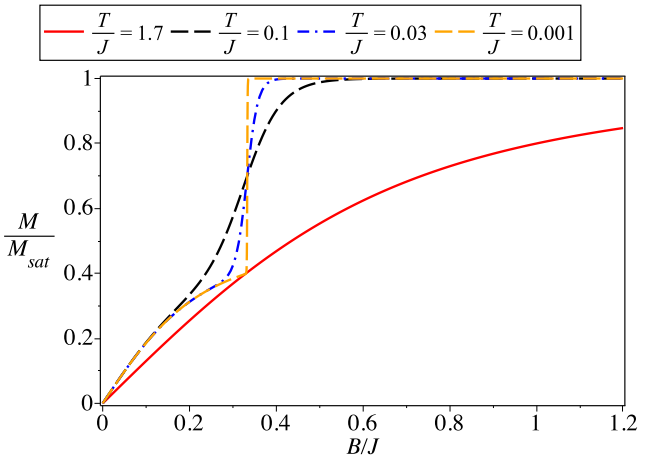

FIG. 4. (Color online) The normalized finite-temperature magnetization curves $M/M_{\rm sat}$ for the $S = 1/2$ spin dimer with two different g factors in the case of isotropic exchange interaction, $\gamma = 0$ and $\Delta = 1$ at different temperatures for $g_1 = 2$, $g_2 = 6$, $J = 1$, $D_z = 0$. $T/J = 1.7$ (red, solid); $T/J = 0.1$ (black, dashed); $T/J = 0.03$ (blue, dot-dashed); and $T/J = 0.001$ (orange, dashed). $M_{\rm sat} = \frac{1}{2}(g_1 + g_2) = 4$.

the spin-1/2 and spin-1 magnetic ions, Δ is an exchange anisotropy in this interaction, D is a uniaxial single-ion anisotropy acting on a spin-1 magnetic ion, and g_1 and g_2 are Landé g factors of the spin-1/2 and spin-1 magnetic ions in an external magnetic field B. As the effect of the XY anisotropy was described in detail in the previous section, here to put it simply, we assume $\gamma = 0$. A straightforward diagonalization of the Hamiltonian (23) gives a full spectrum of eigenstates, which can be characterized by the following set of eigenvalues:

$$\begin{aligned}
\varepsilon_{1,2} &= \frac{1}{2}J\Delta + D \mp \frac{B}{2}(g_1 + 2g_2),\\
\varepsilon_{3,4} &= -\frac{1}{4}(J\Delta - 2D + 2g_2B) \mp \frac{1}{4}\sqrt{(J\Delta - 2D - 2g_-B)^2 + 8J^2},\\
\varepsilon_{5,6} &= -\frac{1}{4}(J\Delta - 2D - 2g_2B) \mp \frac{1}{4}\sqrt{(J\Delta - 2D + 2g_-B)^2 + 8J^2},
\end{aligned} \tag{24}$$

and the corresponding eigenvectors

$$\begin{aligned}
|\Psi_{1,2}\rangle &= \left|\mp\tfrac{1}{2},\mp 1\right\rangle,\\
|\Psi_{3,4}\rangle &= c_1^\pm\left|-\tfrac{1}{2},1\right\rangle \mp c_1^\mp\left|\tfrac{1}{2},0\right\rangle,\\
|\Psi_{5,6}\rangle &= c_2^\pm\left|\tfrac{1}{2},-1\right\rangle \mp c_2^\mp\left|-\tfrac{1}{2},0\right\rangle,
\end{aligned} \tag{25}$$

where the respective probability amplitudes are given by

$$\begin{aligned}
c_1^\pm &= \sqrt{\frac{1}{2}\left[1 \pm \frac{J\Delta - 2D - 2g_-B}{\sqrt{(J\Delta - 2D - 2g_-B)^2 + 8J^2}}\right]},\\
c_2^\pm &= \sqrt{\frac{1}{2}\left[1 \pm \frac{J\Delta - 2D + 2g_-B}{\sqrt{(J\Delta - 2D + 2g_-B)^2 + 8J^2}}\right]}.
\end{aligned} \tag{26}$$

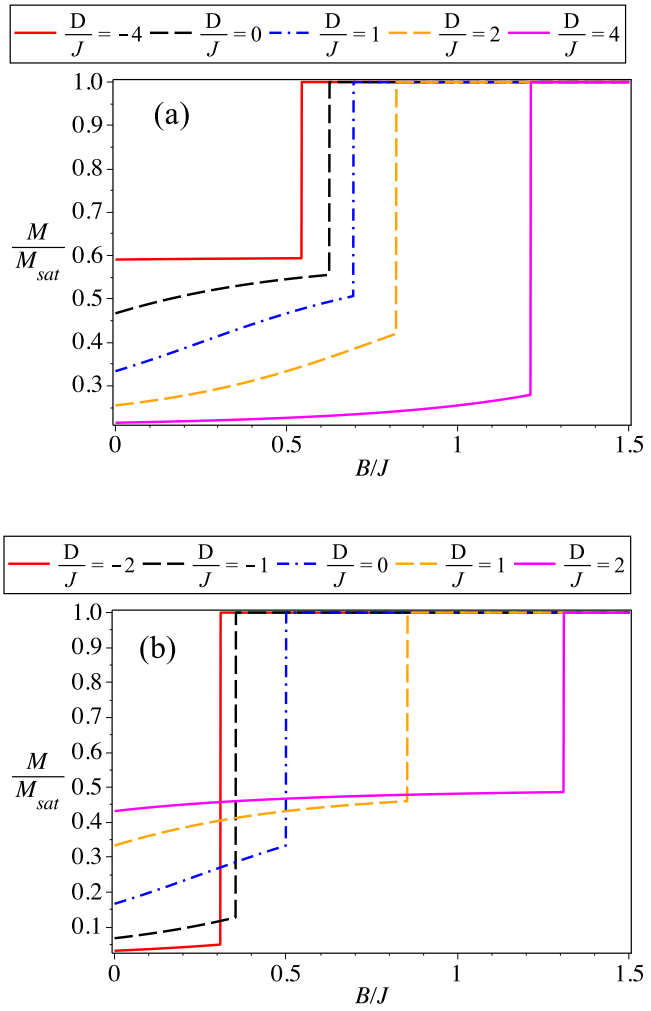

FIG. 5. (Color online) Zero-temperature normalized magnetization curves of the mixed spin-(1/2,1) dimer by assuming the isotropic Heisenberg coupling $\Delta = 1$, several values of the uniaxial single-ion anisotropy, and two different sets of the Landé g factors: (a) $g_1 = 2$, $g_2 = 4$; (b) $g_1 = 4$, $g_2 = 2$. $M_{\rm sat} = \frac{1}{2}(g_1 + 2g_2)$.

It should be mentioned that the mixed spin-(1/2,1) Heisenberg dimer exhibits a strict intermediate plateau at one-third of the saturation magnetization, regardless of uniaxial single-ion anisotropy, on the assumption that the Landé g factors of both constituent magnetic ions are equal, $g_1 = g_2$. If the Landé g factors are different, $g_1 \neq g_2$, then the mixed spin-(1/2,1) Heisenberg dimer displays more intriguing zero-temperature magnetization curves basically affected by a relative strength of the uniaxial single-ion anisotropy. To illustrate the case, the total normalized magnetization of the mixed spin-(1/2,1) dimer is plotted in Fig. 5 against the magnetic field for the isotropic Heisenberg coupling $\Delta = 1$, several values of the uniaxial single-ion anisotropy, and two particular sets of Landé g factors. A smooth variation of the total magnetization observed below a saturation field relates to a gradual change of probability amplitudes of two entangled microstates $|-1/2,1\rangle$ and $|1/2,0\rangle$ within the eigenstate $|\Psi_3\rangle$. In a low-field region with continuously varying magnetization, mean values of two constituent spins and the total magnetization can therefore be calculated with the help of the corresponding lowest-energy eigenvector $|\Psi_3\rangle$ given by Eq. (25):

$$\langle\Psi_3|S_1^z|\Psi_3\rangle = -\frac{1}{2}\frac{J\Delta - 2D - 2g_-B}{\sqrt{(J\Delta - 2D - 2g_-B)^2 + 8J^2}},$$

$$\langle\Psi_3|\mu_2^z|\Psi_3\rangle = \frac{1}{2}\left[1 + \frac{J\Delta - 2D - 2g_-B}{\sqrt{(J\Delta - 2D - 2g_-B)^2 + 8J^2}}\right],$$

$$M = \langle\Psi_3|\left(g_1 S_1^z + g_2\mu_2^z\right)|\Psi_3\rangle = \frac{g_2}{2} - \frac{g_-}{2}\frac{J\Delta - 2D - 2g_-B}{\sqrt{(J\Delta - 2D - 2g_-B)^2 + 8J^2}}. \quad (27)$$

At $g_- = 0$ we have here $M = \frac{g}{2}$ ($g_1 = g_2 = g$). It can be seen from Fig. 5 that the respective field variations of the total magnetization [normalized by the saturation magnetization $M_{\rm sat} = \frac{1}{2}(g_1 + 2g_2)$] depend basically on whether the Landé g factor of the spin-1 magnetic ion is greater or smaller than the g factor of the spin-1/2 magnetic ion. The total magnetization is gradually suppressed by an increase in the single-ion anisotropy in the former case $g_1 < g_2$ [see Fig. 5(a)], while the total magnetization is conversely enhanced by an increase in the single-ion anisotropy in the latter case $g_1 > g_2$ [see Fig. 5(b)]. In general, the total magnetization displays a considerable dependence on a magnetic field for small enough single-ion anisotropies $D/J \approx 0$, while one recovers a quasiplateau dependence with only a subtle variation of the total magnetization in two limiting cases $D/J \to \pm\infty$ at which the following asymptotic values are reached:

$$\lim_{D/J\to\infty} M/M_{\rm sat} = \frac{g_1}{2g_2 + g_1},$$
$$\lim_{D/J\to-\infty} M/M_{\rm sat} = \frac{2g_2 - g_1}{2g_2 + g_1}. \quad (28)$$

However, the most surprising zero-temperature dependence of the total magnetization can be found when the g factor of the spin-1/2 magnetic ion is much greater than the g factor of the spin-1 magnetic ion ($g_1 \gg g_2$) and the uniaxial single-ion anisotropy is of easy-axis type $D < 0$. It turns out that the eigenvector $|\Psi_5\rangle$, characterized by a quantum entanglement of two microstates $|1/2,-1\rangle$ and $|-1/2,0\rangle$, may eventually become the lowest-energy eigenstate with a positive value of the total magnetization, in spite of negative value of the total spin $S_{\rm tot}^z = -1/2$. It is quite evident that a strong enough easy-axis single-ion anisotropy suppresses the occurrence probability of the microstate $|-1/2,0\rangle$, whereas the other microstate $|1/2,-1\rangle$ may lead to a positive magnetization due to the much greater Landé g factor of the spin-1/2 magnetic ion $g_1 \gg g_2$ than that of the spin-1 magnetic ion. Mean values of two constituent spins and the total magnetization follow from the corresponding lowest-energy eigenvector $|\Psi_5\rangle$ given by Eq. (25):

$$\langle\Psi_5|S_1^z|\Psi_5\rangle = \frac{1}{2}\frac{J\Delta - 2D + 2g_-B}{\sqrt{(J\Delta - 2D + 2g_-B)^2 + 8J^2}},$$

$$\langle\Psi_5|\mu_2^z|\Psi_5\rangle = -\frac{1}{2}\left[1 + \frac{J\Delta - 2D + 2g_-B}{\sqrt{(J\Delta - 2D + 2g_-B)^2 + 8J^2}}\right], \quad (29)$$

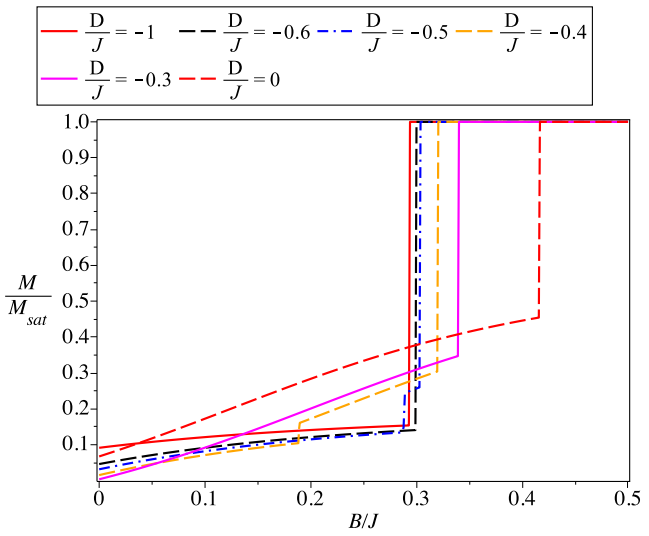

FIG. 6. (Color online) Zero-temperature normalized magnetization curves of the mixed spin-(1/2,1) dimer by assuming the isotropic Heisenberg coupling $\Delta = 1$, several values of the uniaxial single-ion anisotropy, and the Landé g factors $g_1 = 6$ and $g_2 = 2$. $M_{\rm sat} = \frac{1}{2}(g_1 + 2g_2)$.

$$M = \langle\Psi_5|\left(g_1 S_1^z + g_2\mu_2^z\right)|\Psi_5\rangle = -\frac{g_2}{2} + \frac{g_-}{2}\frac{J\Delta - 2D - 2g_- B}{\sqrt{(J\Delta - 2D - 2g_- B)^2 + 8J^2}}. \quad (30)$$

In analogy with the $|\Psi_3\rangle$ case, here we get $M = -\frac{g}{2}$ at $g_1 = g_2 = g$. The zero-temperature magnetization curves displayed in Fig. 6 afford a convincing proof that the total magnetization may vary continuously in a low-field region, and then it may show an abrupt jump to an intermediate-field region with another continuously varying magnetization terminating just at the saturation field. (See the magnetization curves for $D/J = -0.4$ and -0.5.) In accordance with the previous argumentation, the total magnetization follows the formula (30) in the low-field region attributable to the eigenstate $|\Psi_5\rangle$, while it varies according to Eq. (27) in the intermediate-field region attributable to the eigenstate $|\Psi_3\rangle$. The magnetization part corresponding to the eigenstate $|\Psi_3\rangle$ gradually diminishes as the easy-axis single-ion anisotropy strengthens (i.e., it becomes more negative), and hence, the total magnetization shows, below a saturation field, only a single region with continuously varying magnetization due to the striking lowest-energy eigenstate $|\Psi_5\rangle$ with a negative total spin but a positive total magnetization. (See the magnetization curves for $D/J = -0.6$ and -1.0.) It is straightforward to calculate the susceptibility for the eigenstates $|\Psi_3\rangle$ and $|\Psi_5\rangle$:

$$\pm\frac{\partial}{\partial B}\langle\Psi_{3,5}|\left(g_1 S_1^z + g_2\mu_2^z\right)|\Psi_{3,5}\rangle = 2g_-^2\frac{(J\Delta - 2D - 2g_- B)^2 + 4J^2}{[(J\Delta - 2D - 2g_- B)^2 + 8J^2]^{3/2}}, \quad (31)$$

which becomes zero only when $g_1 = g_2$ or $D/J \to \infty$ or $\Delta \to \infty$. It has been demonstrated that a smooth variation of the total magnetization at zero temperature within one and the same eigenstate requires a difference between the Landé g factors. From this perspective, our theoretical predictions could be more easily experimentally tested for the mixed spin-(1/2,1) Heisenberg dimer, which represents a plausible model for heterobimetallic dinuclear complexes naturally having two unequal Landé g factors due to two different constituting magnetic ions. While the quasiplateau phenomenon should still remain a rather subtle effect in heterodinuclear complexes composed of Cu^{2+} (spin-1/2) and Ni^{2+} (spin-1) magnetic ions due to a relatively small difference between the g factors not exceeding a few percent [48,49], it should become much more pronounced in heterodinuclear complexes composed of Co^{3+} (spin-1/2) and Ni^{2+} (spin-1) magnetic ions having a much greater difference between g factors (typically $g_{\rm Co} \approx 5.9$ and $g_{\rm Ni} \approx 2.3$) [50–52].

V. SPIN-1/2 HEISENBERG TRIMER

By complicity the next spin system with the different g factors is the triangle with uniform coupling and with only two g factors given by the Hamiltonian:

$$\mathcal{H}_{\rm trim} = J\left(S_1^x S_2^x + S_1^y S_2^y + \Delta S_1^z S_2^z + S_1^x S_3^x + S_1^y S_3^y + \Delta S_1^z S_3^z + S_2^x S_3^x + S_2^y S_3^y + \Delta S_2^z S_3^z\right) - g_1 B S_1^z - g_2 B\left(S_2^z + S_3^z\right). \quad (32)$$

The Hamiltonian can be diagonalized in a straightforward way. The eigenvalues are

$$\begin{aligned}
\varepsilon_{1,2} &= \frac{3J}{4} \mp \frac{1}{2}(g_1 + 2g_2)B,\\
\varepsilon_{3,4} &= -\frac{J}{4}(2 + \Delta) \mp \frac{1}{2}g_1 B,\\
\varepsilon_{5,6} &= \frac{J}{4}(1 - \Delta) \pm Q_+ + \frac{1}{2}g_2 B,\\
\varepsilon_{7,8} &= \frac{J}{4}(1 - \Delta) \pm Q_- - \frac{1}{2}g_2 B,
\end{aligned} \quad (33)$$

where

$$Q_\pm = \tfrac{1}{2}\sqrt{2J^2 + (J \pm g_- B)^2}. \quad (34)$$

The eigenvectors are

$$\begin{aligned}
&|\Psi_1\rangle = |\uparrow\uparrow\uparrow\rangle,\ \ |\Psi_2\rangle = |\downarrow\downarrow\downarrow\rangle,\\
&|\Psi_3\rangle = |\uparrow\rangle_1|S\rangle_{23},\ \ |\Psi_4\rangle = |\downarrow\rangle_1|S\rangle_{23},\\
&|\Psi_{5,6}\rangle = \frac{1}{\sqrt{2 + c_\pm^2}}(\sqrt{2}|\uparrow\rangle_1|T_0\rangle_{23} + c_\pm|\downarrow\rangle_1|T_+\rangle_{23}),\\
&|\Psi_{7,8}\rangle = \frac{1}{\sqrt{2 + \bar{c}_\pm^2}}(\sqrt{2}|\downarrow\rangle_1|T_0\rangle_{23} + \bar{c}_\pm|\uparrow\rangle_1|T_-\rangle_{23}),
\end{aligned} \quad (35)$$

where the number in the lower-right angle of the symbol $|\rangle$ corresponds to the certain spin in the triangle, and $|S\rangle$, $|T_\pm\rangle$, and $|T_0\rangle$ are spin singlet and components of the spin triplet:

$$|S\rangle = \frac{1}{\sqrt{2}}(|\uparrow\downarrow\rangle - |\downarrow\uparrow\rangle),\quad |T_+\rangle = |\uparrow\uparrow\rangle,\quad |T_-\rangle = |\downarrow\downarrow\rangle,\quad |T_0\rangle = \frac{1}{\sqrt{2}}(|\uparrow\downarrow\rangle + |\downarrow\uparrow\rangle). \quad (36)$$

And the coefficients are

$$c_\pm = \frac{-J\Delta + 2g_- B \pm Q_+}{J\Delta}, \qquad \bar{c}_\pm = \frac{-J\Delta - 2g_- B \pm Q_-}{J\Delta}. \tag{37}$$

For our purposes the eigenvectors from $|\Psi_5\rangle$ to $|\Psi_8\rangle$ are of special interest, as they demonstrate the monotonous explicit dependence of the magnetization on the magnetic field under constant value of the projection of the total spin, which is $\pm\frac{1}{2}$ in our case. The expectation value of the magnetic moment for the eigenstate with the lowest energy among the others ($|\Psi_8\rangle$ for positive B) is

$$\langle\Psi_8|\{g_1 S_1^z + g_2(S_2^z + S_3^z)\}|\Psi_8\rangle = \frac{1}{2}\frac{2g_1 - (g_1 - 2g_2)\bar{c}_-^2}{2 + \bar{c}_-^2}. \tag{38}$$

It is easy to see that for the case of the uniform g factors, $g_1 = g_2 = g$, the magnetic moment expectation value becomes a constant equal to $g/2$. Although, for the eigenvalues of the magnetization operator the limit $g_- = 0$ gives the correct result, this is not the case for the eigenvectors of the Hamiltonian. Thus, one cannot obtain the standard basis for the spin trimer by putting $g_1 = g_2$ in Eqs. (35). The susceptibility for the continuous magnetization (38) is given by

$$\frac{\partial}{\partial B}\langle\Psi_8|\{g_1 S_1^z + g_2(S_2^z + S_3^z)\}|\Psi_8\rangle = -\frac{4g_-\bar{c}_-}{(2+\bar{c}_-^2)^2}\frac{d\bar{c}_-^2}{d\,B}. \tag{39}$$

The susceptibility becomes zero at $g_1 = g_2$. The partition function for the spin trimer under consideration can be obtained in a straightforward way:

$$Z_{\rm trim} = 2e^{\beta\frac{J}{4}}\left\{e^{-\beta J}\,\mathrm{ch}\left(\beta\frac{(g_1+2g_2)B}{2}\right) + e^{\beta\frac{J\Delta}{2}}\,\mathrm{ch}\left(\beta\frac{g_1 B}{2}\right) + e^{-\beta\frac{J\Delta}{4}}\left[e^{-\beta\frac{g_2 B}{2}}\,\mathrm{ch}(\beta Q_+) + e^{\beta\frac{g_2 B}{2}}\,\mathrm{ch}(\beta Q_-)\right]\right\} \tag{40}$$

The finite-temperature magnetization reads

$$M_{\rm trim} = \frac{e^{\beta\frac{J}{4}}}{Z_{\rm trim}}\left\{(g_1+2g_2)e^{-\beta J}\,\mathrm{sh}\left(\beta\frac{(g_1+2g_2)B}{2}\right) + g_1 e^{\beta\frac{J\Delta}{2}}\,\mathrm{sh}\left(\beta\frac{g_1 B}{2}\right) + e^{-\beta\frac{J\Delta}{4}}\left[e^{\beta\frac{g_2 B}{2}}\left(g_2\,\mathrm{ch}\,(\beta Q_-) - \frac{g_-(J-2g_-B)}{Q_-}\,\mathrm{sh}\,(\beta Q_-)\right) - e^{-\beta\frac{g_2 B}{2}}\left(g_2\,\mathrm{ch}\,(\beta Q_+) - \frac{g_-(J+2g_-B)}{Q_+}\,\mathrm{sh}\,(\beta Q_+)\right)\right]\right\}. \tag{41}$$

The plots of the normalized zero-temperature magnetization are presented in Fig. 7. Here the development of the nonplateau part of the magnetization curve with the increase in the difference $g_2 - g_1$ is clearly visible. For comparison, the ordinary curve for $g_1 = g_2$ is also presented with a plateau at $M/M_{\rm sat} = 1/3$, which corresponds to the ground state with $S_{\rm tot}^2 = 3/4, S_{\rm tot}^z = 1/2$:

$$\frac{1}{\sqrt{3}}(|\uparrow\uparrow\downarrow\rangle + |\uparrow\downarrow\uparrow\rangle + |\downarrow\uparrow\uparrow\rangle), \tag{42}$$

which transforms into the $|\Psi_8\rangle$ at $g_2 \neq g_1$. Let us mention also that the $B = 0$ ground state for $g_1 = g_2$ is fourfold degenerate and the magnetic field lifts this degeneracy just partly, because the $1/3$ plateau state is still twofold degenerate. The deviation from the horizontal line becomes more pronounced with the growing difference between g factors of the spins. Thus, the zero-temperature magnetization curve for the simple system with a finite discrete spectrum mimics the magnetic behavior of magnets with the band of magnetic excitations. The value of the critical field at which the level crossing between $|\Psi_8\rangle$ and the fully polarized state $|\Psi_1\rangle$ takes place is

$$B_c = J\frac{2g_+\Delta - g_1 + \sqrt{(2g_-\Delta - g_1)^2 + 8g_1 g_2}}{4g_1 g_2}. \tag{43}$$

In the limit $g_1 = g_2 = g$, the value of critical field is $J\frac{1+2\Delta}{2g}$. The interplay between thermal fluctuations and the nonplateau behavior can be seen in Fig. 8, where one can see a gradual

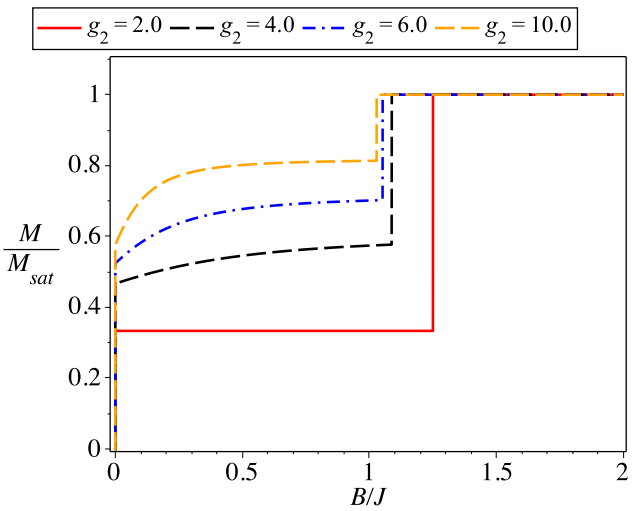

FIG. 7. (Color online) The zero-temperature normalized magnetization curves for the Heisenberg spin trimer with two different Landé g factors for $J = 1$, $\Delta = 2$, $g_1 = 2$, and $g_2 = 2$ (red, solid); $g_2 = 4$ (black, dashed); $g_2 = 6$ (blue, dot-dashed); and $g_2 = 10$ (orange, dashed). $M_{\rm sat} = \frac{1}{2}(g_1 + 2g_2)$.

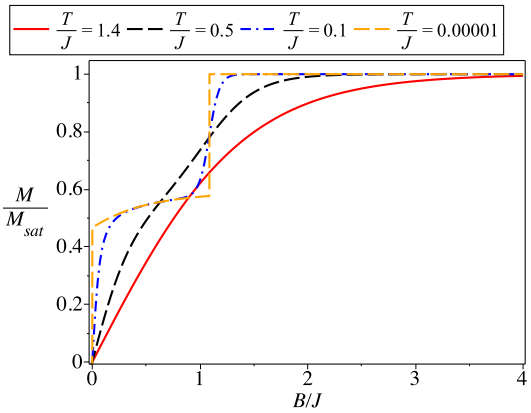

FIG. 8. (Color online) Finite-temperature normalized magnetization curve for the Heisenberg spin trimer with two different Landé g factors for $J = 1$, $\Delta = 2$, $g_1 = 2$, $g_2 = 4$, and $T = 1.4J$ (red, solid); $T = 0.5J$ (black, dashed); $T = 0.1J$ (blue, dot-dashed); and $T = 0.000\,01J$ (orange, dashed). $M_{\rm sat} = \frac{1}{2}(g_1 + 2g_2) = 5$.

smearing out of the magnetization curve with the rise of the temperature.

VI. ISING-HEISENBERG (ISING-XYZ) DIAMOND CHAIN WITH DIFFERENT LANDÉ g FACTORS

To illustrate the features of having the spin cluster with nonconserving magnetization as a constituent of the Ising-Heisenberg one-dimensional systems, let us now consider the simplest Ising-Heisenberg spin chain with the XYZ dimers and different g factors, the diamond chain [14–28]. However, we are not going to describe the entire problem in detail; this can be a topic of a forthcoming and separate investigation. We just want to illustrate how rich the structure of the magnetization curve can be, if we include the spin cluster with nonconserved magnetization into the more involved structures. The interest toward the diamond chain is large not only because of the simplicity of the system, especially in case of Ising-Heisenberg one-dimensional systems, but also as the diamond chain is believed to be the real magnetic structure of the mineral azurite [53–56]. The lattice is depicted in Fig. 9, where the quantum spin dimer is the vertical bonds (solid lines) while the dashed lines correspond to Ising couplings. The Hamiltonian for the whole chain is the sum over the block Hamiltonians:

$$\mathcal{H}_{dc} = \sum_{j=1}^{N} \left\{ \mathcal{H}_j - \frac{B}{2}(g_j\sigma_j + g_{j+1}\sigma_{j+1}) \right\},$$

$$\begin{aligned}\mathcal{H}_j = {} & J\left\{(1+\gamma)S^x_{j,1}S^x_{j,2} + (1-\gamma)S^y_{j,1}S^y_{j,2} + \Delta S^z_{j,1}S^z_{j,2}\right\} \\ & + (K(\sigma_j + \sigma_{j+1}) - g_1 B)S^z_{j,1} \\ & + (K(\sigma_j + \sigma_{j+1}) - g_2 B)S^z_{j,2}, \end{aligned} \tag{44}$$

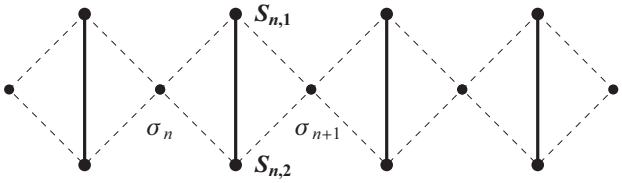

FIG. 9. The Ising-Heisenberg diamond chain. Solid lines represent the quantum interactions, while the dotted ones stand for the interaction involving only z components of the spins. Here we also consider the g factors of the quantum spins $\mathbf{S}_{j,1}$ and $\mathbf{S}_{j,2}$ to be g_1 and g_2, respectively.

where the g factors of the Ising intermediate spins alternating with the spin dimer are also taken alternating

$$g_j = \begin{cases} g_3, & j \text{ is odd} \\ g_4, & j \text{ is even.} \end{cases} \tag{45}$$

A. Exact solution

One can apply the standard technique of the generalized classical transfer matrix to calculate the free energy of the model under consideration exactly [16,18,22,29–31,35,36,42]. However, as here we deal with the alternation of two kind of blocks, one has to compose a two-block transfer matrix just by multiplying transfer matrices for odd and even blocks. In other words, the partition function of the model can be factorized in the following form (the cyclic boundary conditions are assumed):

$$\begin{aligned}\mathcal{Z}_{dc} &= \sum_{\sigma_1,\ldots\sigma_N} \prod_{j=1}^{N} e^{\beta\frac{B}{2}(g_j\sigma_j + g_{j+1}\sigma_{j+1})}\ \mathrm{Tr}_j\ e^{-\beta\mathcal{H}_j(\sigma_j,\sigma_{j+1})} \\ &= \sum_{\sigma_1,\ldots\sigma_N} V_{\sigma_1,\sigma_2}\ V^T_{\sigma_2,\sigma_3}\ldots V^T_{\sigma_N,\sigma_1}, \end{aligned} \tag{46}$$

where with the aid of the block Hamiltonian eigenvalues from Eq. (8), one can obtain four quantities $V_{\sigma_j,\sigma_{j+1}}$, $\sigma_j,\sigma_{j+1} = \pm 1/2$, as the entries of the following matrix:

$$\mathbf{V} = 2e^{-\beta\frac{J\Delta}{4}} \begin{pmatrix} e^{\beta\frac{B(g_3+g_4)}{4}}U_- & e^{\beta\frac{B(g_3-g_4)}{4}}U_0 \\ e^{-\beta\frac{B(g_3-g_4)}{4}}U_0 & e^{-\beta\frac{B(g_3+g_4)}{4}}U_+ \end{pmatrix}, \tag{47}$$

where

$$\begin{aligned} U_\pm &= W + \mathrm{ch}\left(\frac{\beta}{2}\sqrt{(Bg_+ \pm 2K)^2 + J^2\gamma^2}\right), \\ U_0 &= W + \mathrm{ch}\left(\frac{\beta}{2}\sqrt{B^2g_+^2 + J^2\gamma^2}\right), \\ W &= e^{\beta\frac{J\Delta}{2}}\,\mathrm{ch}\left(\frac{\beta}{2}\sqrt{B^2g_-^2 + J^2}\right). \end{aligned} \tag{48}$$

Thus, the partition function can be rewritten in the form

$$\mathcal{Z}_{dc} = 4^{\frac{N}{2}} e^{-\beta\frac{J\Delta N}{4}}\ \mathrm{Tr}\ \mathbf{T}^{\frac{N}{2}}, \tag{49}$$

where,

$$\mathbf{T} = \begin{pmatrix} e^{\beta\frac{B(g_3+g_4)}{2}}U_-^2 + e^{\beta\frac{B(g_3-g_4)}{2}}U_0^2 & \left\{e^{\beta\frac{Bg_4}{2}}U_- + e^{-\beta\frac{Bg_4}{2}}U_+\right\}U_0 \\ \left\{e^{\beta\frac{Bg_4}{2}}U_- + e^{-\beta\frac{Bg_4}{2}}U_+\right\}U_0 & e^{-\beta\frac{B(g_3+g_4)}{2}}U_+^2 + e^{-\beta\frac{B(g_3-g_4)}{2}}U_0^2 \end{pmatrix}.$$

Then, for the free energy per unit cell in the thermodynamic limit, $N \to \infty$, we have

$$f = \frac{J\Delta}{4} - \frac{1}{2\beta}(\log 4 + \log \lambda), \tag{50}$$

where the λ is the largest eigenvalue of the matrix $\mathbf{T}$, which is expressed by the entries of the matrix $\mathbf{T}$ in the following form:

$$\lambda = \frac{1}{2}\left(T_{\frac{1}{2},\frac{1}{2}} + T_{-\frac{1}{2},-\frac{1}{2}} + \sqrt{\left(T_{\frac{1}{2},\frac{1}{2}} - T_{-\frac{1}{2},-\frac{1}{2}}\right)^2 + 4T^2_{\frac{1}{2},-\frac{1}{2}}}\right). \tag{51}$$

Now, we will analyze the nonplateau magnetization for Ising-XYZ diamond chain with different g factors. Using the free energy, one gets the magnetization

$$M = -\left(\frac{\partial f}{\partial B}\right)_\beta = \frac{1}{2\beta}\frac{1}{\lambda}\left(\frac{\partial \lambda}{\partial B}\right)_\beta. \tag{52}$$

As the lattice has six spins in the translational invariant unit cell, two σ spins and two vertical dimers, the total saturation magnetization per one block (note that N is the number of block which is supposed to be even, while the number of the unit cell with six spins is $N/2$) is

$$M_{\text{sat}} = \tfrac{1}{2}\left(g_1 + g_2 + \tfrac{1}{2}(g_3 + g_4)\right). \tag{53}$$

One can see the plots of the zero-temperature magnetization of the Ising-XYZ diamond chain in Fig. 10. The zero-temperature curves can be obtained as a sufficiently low-temperature limit of the exact expression (52). One can see series of quasiplateau and magnetization jumps which can undergo a certain variation under the changing of the XY anisotropy γ (upper panel) or axial anisotropy Δ (lower panel).

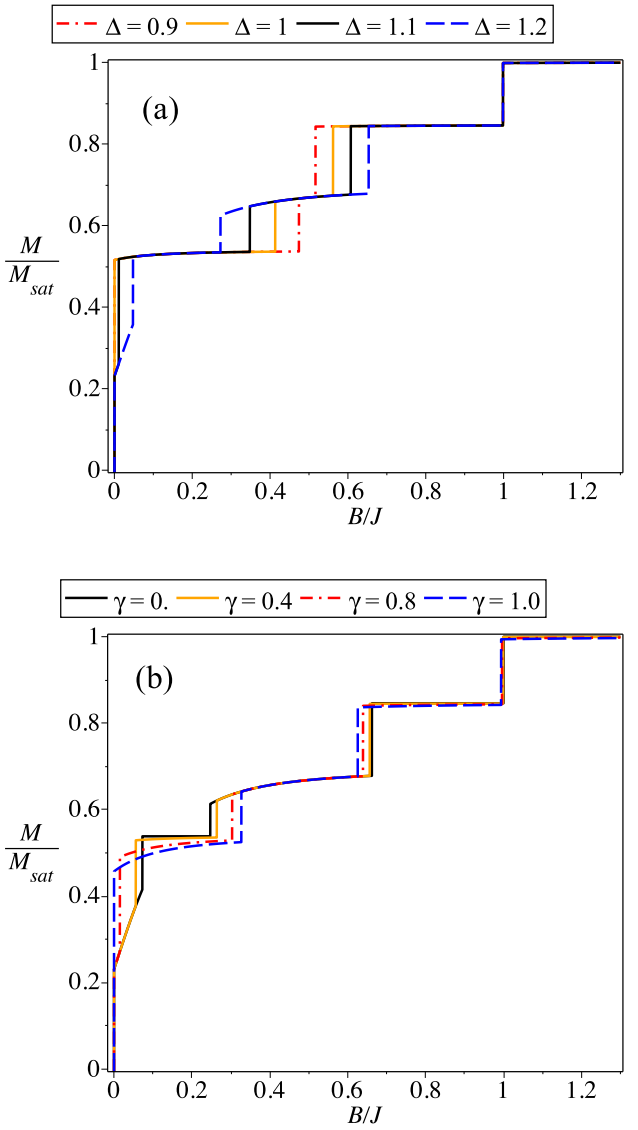

FIG. 10. (Color online) Zero-temperature normalized magnetization as a function of magnetic field. Assuming fixed values: $J = 1, g_1 = 8, g_2 = 2, g_3 = 2, g_4 = 4, K = 1$ (a) for a range values of Δ and fixed $\gamma = 0.5$, and (b) for a range values of γ and fixed $\Delta = 1.2$. $M_{\text{sat}} = \frac{1}{2}[g_1 + g_2 + \frac{1}{2}(g_3 + g_4)] = 13/2$.

B. Ground states

We are not going to present the comprehensive analysis of all possible ground states and all types of magnetization curves for the XYZ-Ising diamond chain with different g factors, but let us just illustrate the ground-state structure of the $T = 0$ magnetization curve from Fig. 10(a). To be specific, let us consider the magnetization curve for $J = 1, K = 1, g_1 = 8, g_2 = 2, g_3 = 2, g_4 = 4, \gamma = 0.5$, and $\Delta = 1.2$. The comparison of the different combinations of the spin-dimer eigenstates [Eq. (9) with $D_z = 0$] with the orientation of the intermediate Ising spins gives rise to a series of possible eigenstates for the chain. However, only a few of them are realized in the case we consider here. First of all, the $B = 0$ ground state is macroscopically degenerate for our choice of parameters. In this ground state all vertical quantum dimers are in $|\Psi_2\rangle$ state from Eq. (9), and all intermediate Ising spins can freely point either up or down. Thus, we have here a 2^N configurations with the same energy. An arbitrary but nonzero magnetic field lifts this degeneracy. The system passes through the following ground state with the increasing magnetic field which corresponds to the course of the magnetization curve we are analyzing here:

$$|GS1\rangle \to |GS2\rangle \to |GS1\rangle \to |GS3\rangle \to |QS\rangle, \tag{54}$$

where the eigenstates with the corresponding magnetization and energies are

$$|GS1\rangle = \prod_{j=1}^{N} |\uparrow\rangle_j \otimes |\Psi_2\rangle_j,$$

$$\mathcal{M}_1 = \frac{Bg_-^2}{2\sqrt{B^2 g_-^2 + J^2}} + \frac{1}{4}(g_3 + g_4),$$

$$E_1 = -\frac{J\Delta}{4} - \frac{1}{2}\sqrt{B^2 g_-^2 + J^2} - \frac{B}{4}(g_3 + g_4),$$

$$|GS2\rangle = \prod_{j=1}^{N} |\downarrow\rangle_j \otimes |\Psi_4^+\rangle_j,$$

$$\mathcal{M}_2 = \frac{g_+(Bg_+ + 2K)}{2\sqrt{(Bg_+ + 2K)^2 + J^2\gamma^2}} - \frac{1}{4}(g_3 + g_4),$$
$$E_2 = \frac{J\Delta}{4} - \frac{1}{2}\sqrt{(Bg_+ + 2K)^2 + J^2\gamma^2} + \frac{B}{4}(g_3 + g_4),$$
$$|GS3\rangle = \prod_{j=1}^{N/2} |\downarrow\rangle_{2j-1} \otimes |\Psi_4\rangle_{2j-1} \otimes |\uparrow\rangle_{2j} \otimes |\Psi_4\rangle_{2j},$$
$$\mathcal{M}_3 = \frac{Bg_+^2}{2\sqrt{B^2g_+^2 + J^2\gamma^2}} - \frac{1}{4}(g_3 - g_4),$$
$$E_3 = \frac{J\Delta}{4} - \frac{1}{2}\sqrt{B^2g_+^2 + J^2\gamma^2} + \frac{B}{4}(g_3 - g_4),$$
$$|QS\rangle = \prod_{j=1}^{N} |\uparrow\rangle_j \otimes |\Psi_4^-\rangle_j,$$
$$\mathcal{M}_{QS} = \frac{g_+(Bg_+ - 2K)}{2\sqrt{(Bg_+ - 2K)^2 + J^2\gamma^2}} + \frac{1}{4}(g_3 + g_4),$$
$$E_{QS} = \frac{J\Delta}{4} - \frac{1}{2}\sqrt{(Bg_+ - 2K)^2 + J^2\gamma^2} - \frac{B}{4}(g_3 + g_4), \tag{55}$$

where $|\Psi_{2,4}\rangle_j$ stands for the corresponding eigenvectors of the spin dimer [Eq. (9) with $D_z = 0$] at the jth block and the $|\Psi_4^{\pm}\rangle_j$ is structurally the same $|\Psi_4\rangle_j$ eigenstate. But taking into account the influence of the interaction with the neighboring Ising spins σ_j and σ_{j+1}, which leads only to a modification of the coefficient B_-,

$$|\Psi_4^{\pm}\rangle = \frac{1}{\sqrt{1 + (B_-^{\pm})^2}}(|\uparrow\uparrow\rangle + B_-^{\pm}|\downarrow\downarrow\rangle),$$
$$B_-^{\pm} = \frac{Bg_+ \pm 2K - \sqrt{(Bg_+ \pm 2K)^2 + J^2\gamma^2}}{J\gamma}, \tag{56}$$

the arrows indicate the orientation of the corresponding Ising spins. Here several comments are in order. First of all, one can see the phenomenon of reentrant phase transition when the system with increasing magnitude of the magnetic field enters the same ground state $|GS1\rangle$ twice. This is also clearly seen from the ground-state phase diagram which is presented in Fig. 11. The return to the ground state $|GS1\rangle$ is possible due to the nonlinear magnetic field dependence of the corresponding magnetization and the energies of all ground states. One can also see from Eq. (55) that despite the visible ideal horizontal character of some part of the magnetization curve, they are not the magnetization plateaus but just the very slowly growing part of the curve. Thus, the magnetization always has an explicit dependence on the magnetic field, unless $\gamma = 0$ or/and $g_1 = g_2$. The quasisaturated state $|QS\rangle$ at finite values of γ has the magnetization asymptotically converging to $M_{\rm sat}$. However, this value is inaccessible for finite values of magnetic field. Although most quasiplateaus appear below the saturation (last critical) field, there also exists an alternative mechanism for quasiplateau formation. Namely, the last plateau emerging above the last critical field (which is in fact not a true saturation field) may change to the quasiplateau due to the XY anisotropy and consequently, the magnetization varies continuously above the last critical field and it never reaches full saturation except for asymptotically infinite magnetic field.

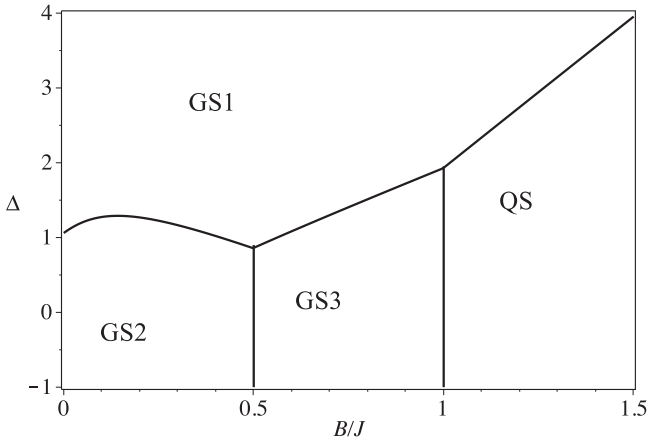

FIG. 11. Zero-temperature ground-state phase diagram Δ versus B/J of the XYZ-Ising diamond chain with the different g factors for $K = 1$, $\gamma = 0.5$ and g factors $g_1 = 8$, $g_2 = 2$, $g_3 = 2$, and $g_4 = 4$.

VII. CONCLUSION

In the present work, we have investigated in detail an absence of actual plateaus in zero-temperature magnetization curves of quantum spin clusters and chains. It has been convincingly evidenced that strict plateaus may disappear from a magnetization process on the assumption that constituent spins of quantum spin clusters have different Landé g factors. More specifically, we have demonstrated this intriguing feature on a few paradigmatic examples of quantum spin clusters such as the spin-1/2 Heisenberg dimer, the mixed spin-(1/2,1) Heisenberg dimer, and the spin-1/2 Heisenberg trimer, whereas the same phenomenon has been also found in the spin-1/2 Ising-Heisenberg diamond chain. From this perspective, the absence of actual magnetization plateaus due to the difference in Landé g factors can be regarded as a general feature of low-dimensional quantum antiferromagnets, because it emerges whenever the total magnetization does not represent a conserved quantity with well-defined quantum spin numbers (the total magnetization need not be proportional to the total spin). Accordingly, a smooth variation of total magnetization can be attributed to a nonlinear dependence of a few (or all) discrete energy levels on a magnetic field.

A few remarks are in order here, which might be useful for possible experimental testing of this interesting phenomenon. Although the magnetization curves of quantum spin clusters without strict plateaus may mimic to a certain extent the magnetization curves of quantum spin chains with continuous energy bands, it is obvious that the absence of magnetization plateaus does not in turn mean a gapless excitation spectrum. On the contrary, small magnetic spin clusters should always have an energy gap, which can be easily experimentally tested by various resonance techniques.

It is also worth noting that the deviation of magnetization from a strict plateau is proportional to a difference between the Landé g factors, which makes an experimental verification of this phenomenon more difficult. As a matter of fact, most

of the transition-metal ions, such as, for instance, Cu^{2+}, Ni^{2+}, Mn^{2+}, Cr^{3+}, or high-spin Fe^{3+} with zero or totally quenched angular momentum, can be described by the notion of more or less isotropic quantum Heisenberg spins and hence, these magnetic ions usually have g factors quite close to the free electron value $g \approx 2$ [50,51,57]. Under these circumstances, it is customary to combine the local Landé g factors of individual magnetic ions into a single molecular g factor as long as the isotropic Heisenberg exchange significantly prevails over the zero-field splitting, asymmetric and/or antisymmetric exchange [58]. Many experimental studies focused on a magnetism of such oligonuclear complexes therefore simply ignore different Landé g factors of individual magnetic ions, as the isotropic exchange is by far the most dominant coupling. However, a few transition-metal ions with unquenched angular momentum may have much higher Landé g factors due to a relatively strong spin-orbit coupling, such as, for example, the low-spin Fe^{3+} ion with a typical value of $g \approx 2.8$ or Co^{2+} ion with $g \approx 6.0$ [50,51,57]. Another possibility as to how to increase the difference of the Landé g factors in oligonuclear complexes is to combine the almost isotropic transition-metal ion with highly anisotropic rare-earth ions, which may even possess much greater Landé g factors (e.g., Dy^{3+} typically has $g \approx 20$), though this extraordinarily large g value usually correlates with a rather strong anisotropy in the exchange interaction [50,59,60]. Under the extreme situation, the XY part of exchange coupling might even be of opposite sign than the Z part (ferromagnetic versus antiferromagnetic), as it has been recently reported for the heterodinuclear Cr^{3+}-Yb^{3+} complex [59].

Last but not least, let us briefly comment on experimental implications for the quantum spin clusters studied in the present work. The spin-1/2 Heisenberg dimer has previously proved its usefulness as the plausible model of many homodinuclear Cu^{2+}-Cu^{2+} complexes [50,51,57,61]. However, the difference between the local Landé g factors in the homodinuclear coordination compounds may only stem from a different coordination sphere of individual magnetic ions, whereas this difference does not exceed in most cases a few percent that would be insufficient for an experimental testing. On the contrary, the considerable difference in the local g factors could be expected in heterobimetallic coordination compounds, which are composed of the nearly isotropic magnetic ion (e.g., Cu^{2+}, Ni^{2+}, high-spin Fe^{3+}, etc.) and the highly anisotropic magnetic ion (e.g., Co^{2+}, low-spin Fe^{3+}, etc.). Hence, the heterodinuclear Co^{2+}-Cu^{2+} and Fe^{3+}-Cu^{2+} complexes could be regarded as sought experimental realizations of the generalized spin-1/2 Heisenberg dimer, which may display a substantial deviation of the magnetization from a strict plateau, as the g factors of individual magnetic ions may even possess opposite signs due to a spin-orbit coupling. (For example, $g_{Fe} \approx -1.7$, $g_{Cu} \approx 2.1$ was reported in Ref. [62], and negative g factors of Co^{2+} and Cu^{2+} magnetic ions were investigated in Ref. [63].) A similar conjecture can be formulated for experimental representatives of the mixed spin-(1/2,1) Heisenberg dimer. As usual, the magnetic anisotropy in heterodinuclear Cu^{2+}-Ni^{2+} complexes does not cause a significant deviation of the magnetization from a strict plateau [48,49], but a rather large deviation could be expected instead in heterodinuclear Co^{2+}-Ni^{2+} coordination compounds with typical values of the g factors $g_{Co} \approx 5.9$ and $g_{Ni} \approx 2.3$ [52]. It can be also anticipated that the homotrinuclear Cu^{2+}-Cu^{2+}-Cu^{2+} complexes [64–66] as experimental representatives of the spin-1/2 Heisenberg trimer should not have a significant deviation of the magnetization from a strict plateau, unlike the heterotrinuclear Cu^{2+}-Co^{2+}-Cu^{2+} complexes [67].

ACKNOWLEDGMENTS

V.O. and J.S. express their gratitude to the LNF-INFN for warm hospitality during work on the project. V.O. also acknowledges partial financial support from the State Committee of Science of Armenia through Grant No. 13-1F343 and from the ICTP Network NET68. J.S. acknowledges financial support from the Scientific Grant Agency of the Ministry of Education of the Slovak Republic under Contracts No. VEGA 1/0234/12 and No. VEGA 1/0331/15. O.R. thanks the Brazilian agencies FAPEMIG and CNPq for partial financial support.

[1] D. C. Mattis, *The Many-Body Problem: An Encyclopedia of Exactly Solved Models in One Dimension* (World Scientific, Singapore, 1993).
[2] S. Katsura, Phys. Rev. **127**, 1508 (1962); **129**, 2835(E) (1963).
[3] P. Pfeuty, Ann. Phys. **57**, 79 (1970).
[4] A. Honecker, J. Schulenburg, and J. Richter, J. Phys.: Condens. Matter **16**, S749 (2004).
[5] *Introduction to Frustrated Magnetism*, edited by C. Lacroix, Ph. Mendels, and F. Mila (Springer, Heidelberg, 2011).
[6] F. D. M. Haldane, Phys. Lett. A **93**, 464 (1983).
[7] F. D. M. Haldane, Phys. Rev. Lett. **50**, 1153 (1983).
[8] M. Oshikawa, M. Yamanaka, and I. Affleck, Phys. Rev. Lett. **78**, 1984 (1997).
[9] I. Affleck, Phys. Rev. B **37**, 5186 (1988).
[10] J. Schnack, Lect. Notes Phys. **645**, 155 (2004).
[11] R. Schmidt, J. Richter, and J. Schnack, J. Magn. Magn. Mater. **295**, 164 (2005).
[12] J. Schnack, Condens. Matter Phys. **12**, 323 (2009).
[13] J. Schnack, J. Chem. Soc., Dalton Trans. **39**, 4677 (2010).
[14] L. Čanová, J. Strečka, and M. Jaščur, J. Phys.: Condens. Matter **18**, 4967 (2006).
[15] L. Čanová, J. Strečka, and T. Lucivjansky, Condens. Matter Phys. **12**, 353 (2009).
[16] O. Rojas, S. M. de Souza, V. Ohanyan, and M. Khurshudyan, Phys. Rev. B **83**, 094430 (2011).
[17] O. Rojas, M. Rojas, N. S. Ananikian, and S. M. de Souza, Phys. Rev. A **86**, 042330 (2012).
[18] S. Bellucci and V. Ohanyan, Eur. Phys. J. B **86**, 408 (2013).
[19] B. Lisnyi and J. Strečka, J. Magn. Magn. Mater. **346**, 78 (2013).
[20] B. Lisnyi and J. Strečka, Phys. Status Solidi B **251**, 1083 (2014).

[21] N. S. Ananikian, J. Strečka, and V. Hovhannisyan, Solid State Commun. **194**, 48 (2014).
[22] J. Torrico, M. Rojas, S. M. de Souza, O. Rojas, and N. S. Ananikian, Europhys. Lett. **108**, 50007 (2014).
[23] E. Faizi and H. Eftekhari, Rep. Math. Phys. **74**, 251 (2014).
[24] Y. Qi and A. Du, Phys. Status Solidi B **251**, 1096 (2014).
[25] B. Lisnyi and J. Strečka, J. Magn. Magn. Mater. **377**, 502 (2015).
[26] V. B. Abgaryan, N. S. Ananikian, L. N. Ananikyan, and V. Hovhannisyan, Solid State Commun. **203**, 5 (2015).
[27] H. Eftekhari and E. Faizi, Chin. Phys. Lett. **32**, 100303 (2015).
[28] K. Gao, Y.-L. Xu, X.-M. Kong, and Z.-Q. Liu, Physica A **429**, 10 (2015).
[29] V. Ohanyan, Condens. Matter Phys. **12**, 343 (2009).
[30] S. Bellucci and V. Ohanyan, Eur. Phys. J. B **75**, 531 (2010).
[31] V. Ohanyan and A. Honecker, Phys. Rev. B **86**, 054412 (2012).
[32] H. G. Paulinelli, S. M. de Souza, and O. Rojas, J. Phys.: Condens. Matter **25**, 306003 (2013).
[33] T. Verkholyak and J. Strečka, Phys. Rev. B **88**, 134419 (2013).
[34] J. S. Valverde, O. Rojas, and S. M. de Souza, J. Phys.: Condens. Matter **20**, 345208 (2008).
[35] D. Antonosyan, S. Bellucci, and V. Ohanyan, Phys. Rev. B **79**, 014432 (2009).
[36] V. Ohanyan, Phys. At. Nucl. **73**, 494 (2010).
[37] O. Rojas, J. Strečka, and M. L. Lyra, Phys. Lett. A **377**, 920 (2013).
[38] J. Strečka, O. Rojas, T. Verkholyak, and M. L. Lyra, Phys. Rev. E **89**, 022143 (2014).
[39] J. Strečka, M. Jaščur, M. Hagiwara, K. Minami, Y. Narumi, and K. Kindo, Phys. Rev. B **72**, 024459 (2005).
[40] D. Visinescu, A. M. Madalan, M. Andruh, C. Duhayon, J.-P. Sutter, L. Ungur, W. Van den Heuvel, and L. F. Chibotaru, Chem. Eur. J. **15**, 11808 (2009).
[41] W. Van den Heuvel and L. F. Chibotaru, Phys. Rev. B **82**, 174436 (2010).
[42] S. Bellucci, V. Ohanyan, and O. Rojas, Europhys. Lett. **105**, 47012 (2014).
[43] K. Penc, J.-B. Fouet, S. Miyahara, O. Tchernyshyov, and F. Mila, Phys. Rev. Lett. **99**, 117201 (2007).
[44] S. Miyahara, J.-B. Fouet, S. R. Manmana, R. M. Noack, H. Mayaffre, I. Sheikin, C. Berthier, and F. Mila, Phys. Rev. B **75**, 184402 (2007).
[45] S. R. Manmana and F. Mila, Europhys. Lett. **85**, 27010 (2009).
[46] M. I. Belinsky, Phys. Rev. B **84**, 064425 (2011).
[47] J. M. Florez and P. Vargas, J. Magn. Magn. Mater. **324**, 83 (2012).
[48] P. Bergerat, O. Kahn, and M. Guillot, Inorg. Chem. **30**, 1966 (1991).
[49] M. Hagiwara, Y. Narumi, K. Minami, K. Tatani, and K. Kindo, J. Phys. Soc. Jpn. **68**, 2214 (1999).
[50] L. J. De Jongh and A. R. Miedema, Adv. Phys. **23**, 1 (1974).
[51] R. L. Carlin, *Magnetochemistry* (Springer-Verlag, Berlin, 1986).
[52] E. Coronado, F. Sapina, M. Drillon, and L. J. de Jongh, J. Appl. Phys. **67**, 6001 (1990).
[53] H. Kikuchi, Y. Fujii, M. Chiba, S. Mitsudo, T. Idehara, T. Tonegawa, K. Okamoto, T. Sakai, T. Kuwai, and H. Ohta, Phys. Rev. Lett. **94**, 227201 (2005).
[54] K. C. Rule, A. U. B. Wolter, S. Süllow, D. A. Tennant, A. Brühl, S. Köhler, B. Wolf, M. Lang, and J. Schreuer, Phys. Rev. Lett. **100**, 117202 (2008).
[55] F. Aimo, S. Krämer, M. Klanjšek, M. Horvatić, C. Berthier, and H. Kikuchi, Phys. Rev. Lett. **102**, 127205 (2009).
[56] A. Honecker, S. Hu, R. Peters, and J. Richter, J. Phys.: Condens. Matter **23**, 164211 (2011).
[57] O. Kahn, *Molecular Magnetism* (VCH, New York, 1991).
[58] R. Boča, Coord. Chem. Rev. **248**, 757 (2004).
[59] V. S. Mironov, L. F. Chibotaru, and A. Ceulemans, Phys. Rev. B **67**, 014424 (2003).
[60] L. F. Chibotaru, in *Molecular Nanomagnets and Related Phenomena*, edited by S. Gao, Structure and Bonding Vol. 164 (Springer-Verlag, Berlin, 2015).
[61] H. Ojima and K. Nonoyama, Coord. Chem. Rev. **92**, 85 (1988).
[62] M. Atanasov, P. Comba, and C. A. Daul, Inorg. Chem. **47**, 2449 (2008).
[63] L. F. Chibotaru and L. Ungur, Phys. Rev. Lett. **109**, 246403 (2012).
[64] K.-Y. Choi, N. S. Dalal, A. P. Reyes, P. L. Kuhns, Y. H. Matsuda, H. Nojiri, S. S. Mal, and U. Kortz, Phys. Rev. B **77**, 024406 (2008).
[65] K. Iida, Y. Qiu, and T. J. Sato, Phys. Rev. B **84**, 094449 (2011).
[66] K. Y. Choi, Z. Wang, H. Nojiri, J. van Tol, P. Kumar, P. Lemmens, B. S. Bassil, U. Kortz, and N. S. Dalal, Phys. Rev. Lett. **108**, 067206 (2012).
[67] N. Fukita, M. Ohba, T. Shiga, H. Okawa, and Y. Ajiro, J. Chem. Soc., Dalton Trans., 64 (2001).